DOI 10.1007/s11182-018-1537-9

Russian Physics Journal, Vol. 61, No. 7, November, 2018 (Russian Original No. 7, July, 2018)

PLASMA PHYSICS

AN INVESTIGATION OF REGULAR PATTERNS OF THE ANODE SPOT GLOW IN A HIGH-CURRENT VACUUM ARC BY THE METHOD OF HIGH-SPEED PHOTOGRAPHY

A. V. Schneider, S. A. Popov, V. A. Lavrinovich, and D. D. Maral UDC 533.9.082.5

The evolution of an anode spot is investigated in the course of burning of a high-current vacuum arc. The evolution process is recorded with a high-speed video camera at a rate of 180 thousand frames per second and with a high-speed 4-channel photo camera, which is equipped with a set of interference filters to register the distribution of Cr I *(428 nm),* Cu II *(625 nm) and* Cr I + Cu II *(500 nm) in the gap. The arc is ignited between two* CuCr-*electrodes measuring 20 mm in diameter in a vacuum arc chute imitating the operation of a vacuum circuit breaker by switch opening at a constant rate.*

Keywords: anode spot, anode plume, high-current vacuum arc, vacuum switch.

INTRODUCTION

It is well known that an anode spot is a high-intensity plasma source, in addition to cathode spots, and a source of electrode material vapors. Due to this it plays a significant role in a high-current vacuum discharge and, among other reasons, contributes to a high-current vacuum breakdown after crossing the current-zero point [1, 2]. An anode spot significantly affects the contact erosion and the interrupting capacity of a vacuum switch [1, 3–5], making this area challenging for research.

Based on the literature data, three types of burning modes of a high-current vacuum arc can be singled out [2, 6, 7]: an intermediate mode of unstable anode spots (so-called footpoint arc), a high-intensity arc (without an anode spot), and an anode-spot arc. Furthermore, in the anode-spot arc two types of spot burning are distinguished [8], which differ in voltage and radiation intensity [9]. The description of an arc in vacuum circuit breakers, ignited by the contact opening followed by their separation and an increase in the current up to a few and tens of amperes, however, involves a more complex arc-mode classification [10]. The anode in all these arc-burning modes is found in an active regime (in contrast to the diffuse mode), emitting a metal vapor flow into the discharge gap. Under the conditions of a rapidly increasing voltage on the gap after the current-zero point, the vapors play a critical role in reconstructing the vacuum insulation, and the switch is characterized by a lower interrupting capacity.

In this study we present sequences of high-speed photographs of an anode spot together with spectrally-selective images of the distributions of chromium atoms and copper ions in the discharge gap.

It is shown that the anode plume reported in [11, 12] can appear and disappear several times during the arc-burning event, which is accompanied by modulations in the voltage oscilloscope trace. The anode plume is generally formed in the descending section of the arc-burning voltage.

Institute of High-Current Electronics of the Siberian Branch of the Russian Academy of Sciences, Tomsk, Russia, e-mail: schneider@lve.hcei.tsc.ru; Popov@lve.hcei.tsc.ru; lavrhome@rambler.ru. Translated from Izvestiya Vysshikh Uchebnykh Zavedenii, Fizika, No. 7, pp. 126–130, July, 2018. Original article submitted April 19, 2018.

EXPERIMENTAL PROCEDURE

The experiments were performed using a Weil – Dobke synthetic circuit [1] capable of imitating the operation of a vacuum arc-quenching chamber (VAQC) of a vacuum circuit breaker in the short-circuiting mode [13]. This circuit is capable of generating a harmonic current pulse with an amplitude of up to 50 kA and a base duration 10 ms, which corresponds to the commercial current frequency 50 Hz. The circuit contains calibrated gages for measuring the arc current and gap voltage.

The experiments were carried out at a residual chamber pressure of $\sim 10^{-5}$ Pa, which was sustained by a Penning-type pump. The arc gap was formed by two identical electrodes 2 cm in diameter. The electrodes were manufactured from a copper-chromium composite CuCr25. The arc discharge was initiated by opening of the contacts. The electrodes were separated at a constant rate of 1 m/s. No external magnetic fields were generated.

A Photron Fastcam SA1.1 high-speed video camera was used for recording the anode spot evolution, whose recording rate depended on the spatial resolution of the frame. A typical recording rate was 180 thousand frames per second at the frame resolution 128×128. An HSFC Pro high-speed 4-channel 12-bit camera, equipped with a PC Micro-NIKKOR lens, was used for recording sequential images during the arc burning event. Spectral-selective images were recorded with a set of interference light filters with the full width at half maximum (FWHM) about 10 nm towards the wavelength range from 350 to 1100 nm at a step of 25 nm. The process was observed through the optical quartz windows of the vacuum chamber.

Recording of the images was accompanied by oscilloscopic sampling of the current and voltage waveforms. The oscilloscope traces and the images were synchronized by the sync pulses of the cameras. The signals were registered by the Tektronix TDS 2000 digital oscilloscopes.

EXPERIMENTAL RESULTS

Typical oscilloscope traces of the arc current and voltage are presented in Fig. 1. From the point of the discharge initiation to the point of time 3.7 ms the arc burns in a diffuse mode. There is no anode glow (Fig. 2*a*). After the point of time 3.7 ms, the diffuse mode transforms into an anode-spot mode, which is accompanied by an increase in the discharge burning voltage (Fig. 1*b*), then a weak glow appears on the anode (Fig. 2*b*). From the point of time 3.7 to 3.8 ms, an anode spot of the first type is observed [14]. From the point of time 3.8 ms and on up to 4 ms (Fig. 1*b*) an anode spot of the second type is observed with more intense glow on the anode followed by the formation of a macrospot [15] on the cathode (Fig. 2*c*). During this period of time, the cathode spots are grouped on the cathode surface forming intense glow in front of the anode spot. Thus, two regions (Fig 2*c*) of high-intensity glow are formed in the interelectrode gap, which are separated by dark space. As this goes on, the discharge voltage increases by 15–20 V very rapidly.

At the point of time 3.98 ms, the discharge burning voltage decreases, the discharge transits into a diffuse mode, the cathode spot disintegrates, and an anode plume is formed. The anode plume is formed quite rapidly. Figure 3 presents a sequence of photographs of the anode plume formation in a high-current vacuum arc with the time reference.

It is clear in Fig. 3 that at the point of time 3.98 ms the discharge was in the mode of the second-type anode spot, and there was a macrospot on the cathode. By the point of time 3.99 ms, the macrospot had disintegrated, and a plume started to form on the anode.

For the registration of spectral-selective images, three different interference filters transmitting light only in a narrow range of about 10 nm were selected for the wavelengths of the Cr I, Cu II and Cr I and Cu II lines simultaneously. While these lines have been chosen merely due to a limited set of light filters available, the Cu I and Cr II lines are also present in the arc formed by the copper-chromium electrodes. The images in Fig. 4 demonstrate that the larger part of the anode plume light is emitted by the excited neutral atoms of chromium, as is the case of plume formation at the end of the current pulse. The anode plume envelope is surrounded by a diffuse halo emitted by the copper atoms [12]. The anode plume formation is due to the collision between a highly ionized cathode plasma and the weakly ionized anode plasma. In this collision, an ionization-recombination front is formed (IRF). The major mechanism of the anode flow ionization is the resonant recharging of ions on atoms. It is the concept of IRF and the

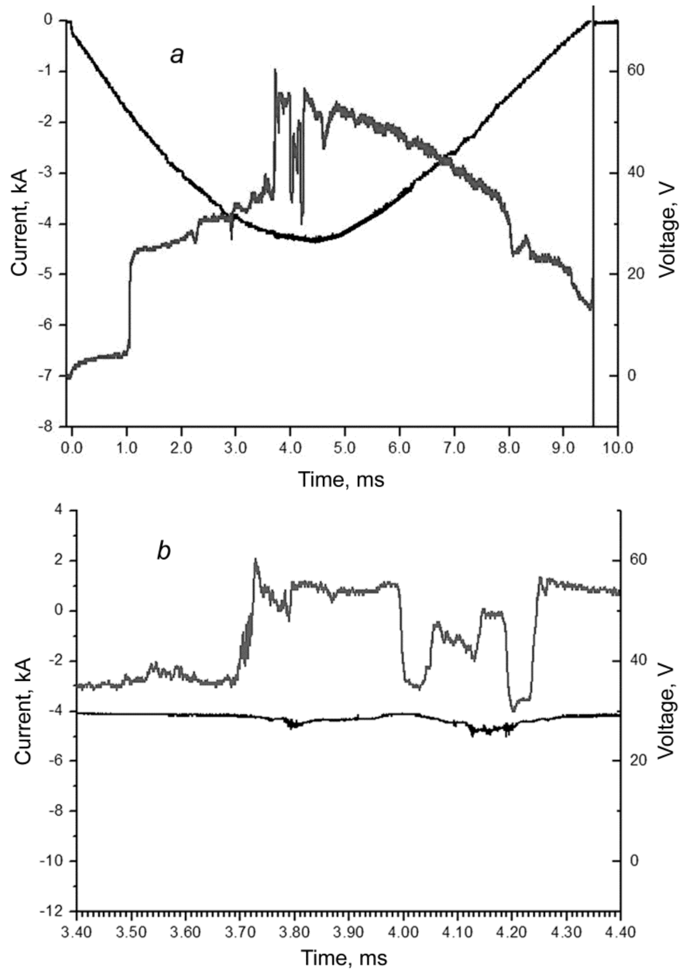

Fig. 1. Overview (*a*) and detailed (*b*) oscilloscope traces of the arc discharge current and voltage.

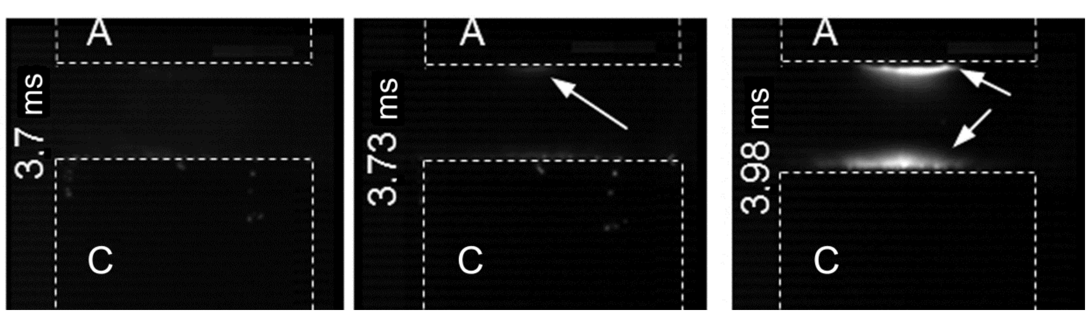

Fig. 2. Transition of the arc discharge from the mode of the first-type anode spot to the second-type anode spot. A – anode, C – cathode.

images obtained which allow estimating the average vapor concentration in the anode plume: emission occurs from a narrow region whose thickness is on the order of $\ell \sim 1$ mm. Recharging takes place at $\ell \approx \sigma^{-1} n_a^{-1}$, where σ is the resonant recharging cross-section (~10^{-14} cm^2) and n_a is the concentration of neutral atoms. In this case $n_a \approx 10^{15}$ cm^{-3}, which corresponds to the vapor pressure about 10 Pa. This estimate is quite reasonable for the conditions of a high-current vacuum arc [12].

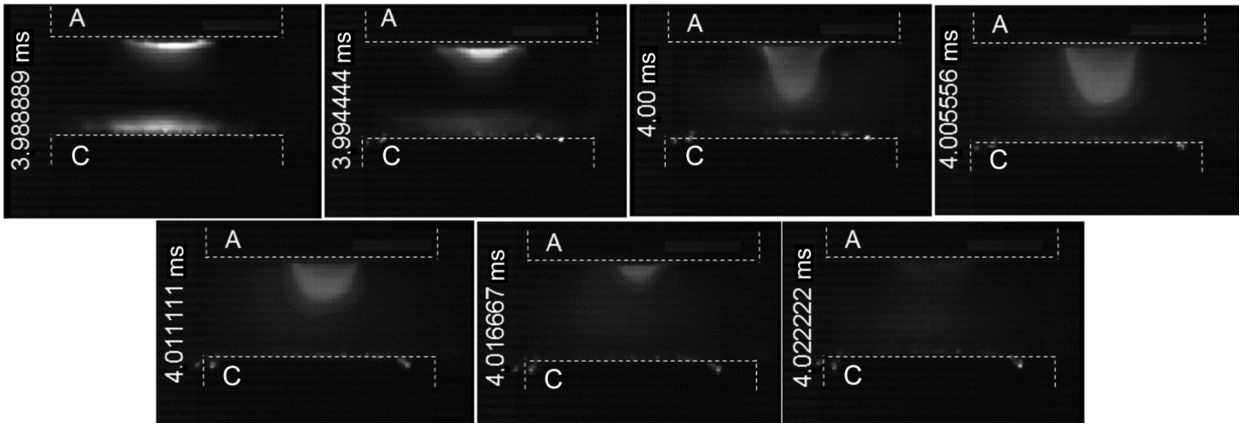

Fig. 3. Frame sequence of the anode plume formation in a high-current vacuum arc at the current amplitude 4 kA: A – anode, C – cathode.

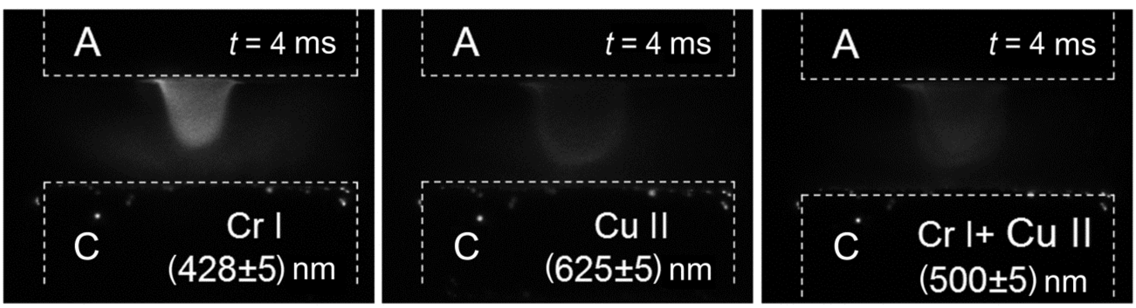

Fig. 4. Simultaneously recorded spectral-selective images of the gap during the arc burning on the CuCr-electrodes obtained at the point of time 4 ms (correspond to the frame in Fig. 3), which match the discharge current ~4 kA. Exposure time: *a* – 2 μs, *b* – 3.6 μs, *c* – 3 μs.

After the formation and decay of the anode plume the discharge again transits into the mode of the second-type anode spot, two macroregions of intense glow are formed from the anode and cathode, and the discharge burning voltage increases (4.06 ms in Fig. 1*b*). This regime is maintained up to the point of time 4.18 ms. Then the gap voltage rapidly drops within 20 μs, which gives rise to the formation of the next anode plume (Fig. 5), appearing, as in the previous case, on the descending part of the voltage trace.

After the formation and decay of a regular anode plume the discharge returns into the anode-spot mode (Fig. 5, time point 4.25 ms) and continues burning in the mode up to 8 ms without any substantial changes. Since the discharge current decreases, the gap voltage gradually drops and the power density delivered to the anode also decreases. The anode gradually cools down and at the time point 8 ms the anode glow disappears, which indicates the discharge transition into a diffuse mode. The diffuse mode is sustained until the arc is interrupted.

SUMMARY

The findings of an investigation of the anode-spot evolution during the event of a high-current vacuum arc burning have been presented.

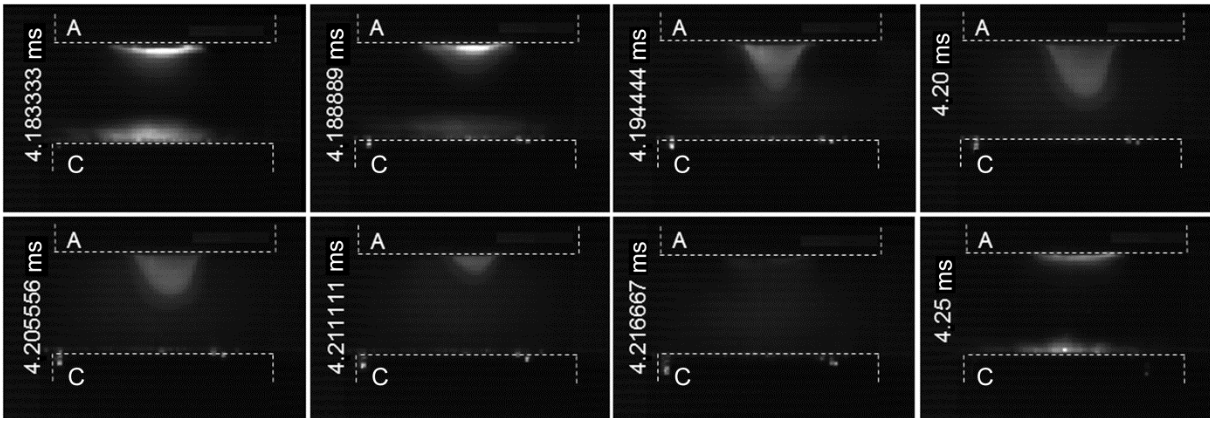

Fig. 5. Frame sequence of the formation of the second anode plume within the time interval 4.18–4.22 ms.

The anode spot evolution has been recorded using a high-speed video camera at rate of 180 thousand f/s and a high-speed 4-channel photo camera equipped with a set of interference filters for registration of the distribution of chromium and copper vapors in the gap.

It has been shown that the burning modes of a high-current vacuum arc can repeatedly change during the arc burning event. A transition from the cathode spot mode is followed by the anode plume formation. The anode plume is formed not only at the end of the current pulse, as it was earlier shown in [12] and later in [14], but it can also be formed time and again during the arc burning event on the descending part of the burning voltage in the case of oscillations caused by the discharge burning instabilities.

The investigation has been funded by a grant of the Russian Science Foundation (Project No. 17-79-20049).

REFERENCES

1. P. G. Slade, The Vacuum Interrupter. Theory, Design, and Application, CRC Press, N. Y. (2008).
2. H. C. Miller, Contrib. Plasma Phys., **29,** No. 3, 223–249 (1989).
3. E. Schade, IEEE Trans. Plasma Sci., **33**, No. 5, 1564–1575 (2005).
4. E. Schade and E. Dullni, IEEE Trans. Dielect. Electr. Insul., **9**, No. 2, 207–215 (2002).
5. E. Dullni and E. Schade, IEEE Trans. Electr. Insul., **28**, No. 4, 607–620 (1993).
6. H. C. Miller, IEEE Trans. Plasma Sci., **11**, No. 2, 76–89 (1983).
7. H. C. Miller, IEEE Trans. Plasma Sci., **11**, No. 3, 122–127 (1983).
8. A. Khakpour *et al.,* IEEE Trans. Plasma Sci., **44**, No. 12, 3337–3345 (2016).
9. A. Khakpour *et al*., IEEE Trans. Plasma Sci., **44**, No. 10, 2462–2469 (2016).
10. J. Heberlein and J. Gorman, IEEE Trans. Plasma Sci., **8**, No. 4, 283–288 (1980).
11. A. V. Batrakov, S. A. Popov, A. V. Schneider, *et al*., IEEE Trans. Plasma Sci., **39**, No. 6, 1291–1295 (2011).
12. S. A. Popov, A. V. Schneider, A. V. Batrakov, *et al*., ZhTF, **82**, Iss. 7, 44– 50 (2012).
13. A. V. Schneider, S. A. Popov, and A. V. Batrakov, Izv. Vyssh. Uchebn. Zaved. Fiz., **56**, No.7/2, 373–378 (2013).
14. A. Khakpour, S. Franke, R. Methling, *et al*., IEEE Trans. Plasma Sci., **45**, No. 8, 2126–2134 (2017).
15. S. Popov, A. Schneider, V. Lavrinovich, *et al*., in: Proc. 27th International Symposium on Discharges and Electrical Insulation in Vacuum (27th ISDEIV) 18–23 Sept. 2016, Suzhou, China (2016).